Solution Behavior of a Random Copolymer of Poly(isobutyl methacrylate-(*tert*-butylamino)ethyl methacrylate). 1. Laser Light Scattering Studies

Benjamin Chu,*,†,‡ Jian Wang,† and Wendel J. Shuely§

Chemistry Department, State University of New York at Stony Brook, Long Island, New York 11794-3400, Department of Materials Science and Engineering, State University of New York at Stony Brook, Long Island, New York 11794-2275, and Research Directorate, Chemical Research, Development, and Engineering Center, Aberdeen Proving Ground, Maryland 21010-5423. *Received June 5, 1989; Revised Manuscript Received September 29, 1989*

ABSTRACT: Laser light scattering studies of solution behavior of a random copolymer of poly(isobutyl methacrylate-*co*-(*tert*-butylamino)ethyl methacrylate) in isopropylamine, *N,N,N',N'*-tetramethylethylenediamine (TMEDA), *N,N*-dimethylformamide, *N,N*-dimethylacetamide, and a 0.4/0.6 (molar ratio) mixture of TMEDA and 3-heptanone are described. By taking advantage of the isorefractive property of poly(isobutyl methacrylate) [poly(iBMA)], poly((*tert*-butylamino)ethyl methacrylate) [poly(tBAEMA)], and poly(iBMA-tBAEMA), the light scattering intensity properties for the copolymer poly(iBMA-tBAEMA) could be approximated as those of a homopolymer. Therefore, a distinguishing characteristic of the copolymer as a polymer additive that can influence the rheology of a large variety of fluids can be attributed to polymer aggregation by intra- and intermolecular interactions.

I. Introduction

Acrylate or methacrylate polymers with pendant aminoalkyl groups have a wide range of applications, such as additives for lubricants, cosmetic preparations, and coatings. Hong and McHugh have made extensive reviews on the preparation and properties of aminoalkyl acrylates and methacrylates[1] and of copolymers from aprotic (acrylic) monomers and protic (acrylic) monomers.[2] The presence of pendant aminoalkyl groups adds cationic characteristics to the copolymer and changes its solubility behavior. Depending on the solvent nature, such copolymers have the potential to exhibit (pseudo) ionomer solution properties involving intramolecular and intermolecular interactions. One consequence of having aprotic/protic (or ionic) pendant groups present in a polymer chain is its ability to be soluble in both nonpolar and polar solvents. But the detailed nature for the solubilization process could be complex and could vary with the solvents. The other property that makes ionomer-like copolymers with pendant aminoalkyl groups as useful polymer additives is their ability to change the viscosity of the fluids. However, an understanding on the macromolecular behavior of such copolymers in solution has lagged far behind the industrial applications. In this paper, we report laser light scattering (LLS) studies on the solution properties of poly(isobutyl methacrylate-*co*-(*tert*-butylamino)ethyl methacrylate), abbreviated as poly(iBMA-tBAEMA), over a broad range of concentrations in several different solvents. In a followup paper we shall present the viscosity studies of poly(iBMA-tBAEMA) solutions.

Light scattering (LS) has been used to determine the molecular weight of synthetic homopolymers for more than 40 years.[3] The theoretical treatment for light scattering by solutions of copolymers was developed by Stockmayer et al.[4] and by Bushuk and Benoit[5] more than 30 years ago. However, only a handful of experiments have been reported since then.[6] The application of light scattering to the absolute molecular weight determination of copolymers has not been popular because of the requirement to use at least three solvents with sufficiently diverse refractive index in order to interpolate (or extrapolate) the true molecular weight from several apparent molecular weight determinations. For a copolymer with protic and aprotic pendant groups, such as poly(iBMA-tBAEMA), solution studies of intramolecular and intermolecular interactions would be very complex if we were to add the problem related to the nonlinear additivity of the refractive index by the homopolymer segments in the copolymer in light scattering intensity measurements.[4,5] Fortunately, homopolymers of poly(iBMA) and poly(tBAEMA) have comparable refractive indices that are essentially the same within the experimental error limits. Thus, we were able to carry out light scattering studies by assuming the copolymer to be a "homopolymer" in terms of its scattering behavior; this isorefractive property of poly(iBMA), poly(tBAEMA), and poly(iBMA-tBAEMA) permits us, for the first time to our knowledge, to investigate the intramolecular and intermolecular interactions of such systems by means of LLS. As the key to our analysis is based on the isorefractive nature of the homopolymers and the copolymer, we have also included an analysis of the effects of small refractive index increment differences to LLS in our discussions.

In the following sections, we summarize the theoretical background in II, experimental methods in III, results and discussion in IV, and conclusions in V.

II. Theoretical Background

II.1. Static Light Scattering. The *excess* Rayleigh ratio R_{vv} for vertically polarized incident and scattered light due to a polydisperse homopolymer of uniform refractive index increment ν ($\equiv(dn/dC)$) has the form

$$\lim_{\substack{C\to 0\\ \theta\to 0}} (H^*C/R_{vv}) = 1/(M_w\nu^2) \qquad (1)$$

where $H^* = 4\pi^2n^2/(N_A\lambda_0^4)$ with n, N_A, and λ_0 being respec-

* Author to whom all requests for reprints should be addressed.
† Chemistry Department, State University of New York at Stony Brook.
‡ Department of Materials Science and Engineering, State University of New York at Stony Brook.
§ Research Directorate, Chemical Research, Development, and Engineering Center.

0024-9297/90/2223-2252$02.50/0

tively the refractive index, the Avogadro number, and the incident wavelength in vacuo; C is the polymer concentration; M_w [$\equiv \sum W_i M_i$ with W_i ($=C_i/C$) and M_i being respectively the weight fraction and the molecular weight of polymer species of chain length i] is the weight-average molecular weight; and θ is the scattering angle. At finite scattering angles with $KR_g \lesssim 1$ and dilute concentrations, eq 1 becomes

$$\frac{HC}{R_{vv}(K)} \simeq \frac{1}{M_w}\left(1 + \frac{K^2 R_g^2(C)}{3}\right) + 2A_2C \qquad (2)$$

where $H = H^*\nu^2$ and K [$=(4\pi/\lambda)\sin(\theta/2)$ with $\lambda = \lambda_0/n$] and A_2 are respectively the magnitude of the momentum transfer vector and the second virial coefficient. $R_g^2(C)$ is an apparent radius of gyration at concentration C with R_g^2 [$=\lim_{C\to 0} R_g^2(C)$] being the mean-square z-average radius of gyration.

For a solution of copolymers with polydisperse chain length and composition, the excess Rayleigh ratio extrapolated to zero scattering angle and concentration, R_{vv}^0, has the form

$$R_{vv}^0 = H^* \sum_i C_i M_i \nu_i^2 \qquad (3)$$

The apparent molecular weight M_{app} corresponds to the intercept in a plot of $\lim_{K\to 0}(HC/R_{vv})$ vs C and can be expressed by

$$M_{app} = \frac{1}{\nu^2}\sum_i W_i M_i \nu_i^2 \qquad (4)$$

where ν is the refractive index increment of the copolymer solution. For each molecular weight M_i, there can be a heterogeneity in composition such that $\nu_i = \sum_j W_{ij}\nu_j$ where we have assumed additivity of refractive index increments of the components (j = A and B) of the copolymer in a specific solvent. By definition, we then have $\nu_i = W_{iA}\nu_A + W_{iB}\nu_B$, $W_{iA} + W_{iB} = 1$, and $W_A + W_B = 1$ and $\delta W_{iA} = -\delta W_{iB}$ with $\delta W_{iA} = W_{iA} - W_A$ and $\delta W_{iB} = W_{iB} - W_B$, yielding

$$M_{app}\left(=\sum_i W_i M_i\left[\frac{W_{iA}\nu_A + W_{iB}\nu_B}{\nu}\right]^2\right) = M_w + 2P\left(\frac{\nu_A - \nu_B}{\nu}\right) + Q\left(\frac{\nu_A - \nu_B}{\nu}\right)^2 \qquad (5)$$

with

$$P = \sum_i W_i M_i \delta W_{iA}$$

$$Q = \sum_i W_i M_i (\delta W_{iA})^2$$

If we let experimental uncertainties in $\nu_A - \nu_B$ be Δ, the measured uncertainty in the molecular weight determination for a copolymer with almost isorefractive homopolymer components becomes

$$\Delta M_w \simeq \Delta M_{app} \simeq 2(P/\nu)\Delta + 2Q(\Delta/\nu)^2 \qquad (6)$$

II.2. Dynamic Light Scattering. The measured photoelectron count autocorrelation function $G^{(2)}(t)$ is related to the normalized electric field autocorrelation function $g^{(1)}(t)$ by the relation

$$G^{(2)}(t) = A(1 + b|g^{(1)}(t)|^2) \qquad (7)$$

where A is the background and b accounts for the nonideal point detector. The net intensity autocorrelation function, $[G^{(2)}(t)/A] - 1 = b|g^{(1)}(t)|^2$, can be related to monodisperse particle translational motions at dilute concentrations such that

$$b|g^{(1)}(t)|^2 = be^{-2\Gamma t} \qquad (8)$$

with $\Gamma = DK^2$ and D being the translational diffusion coefficient. At finite concentrations, we have

$$D^0 = D_0^0(1 + k_d C) \qquad (9)$$

For a polydisperse polymer solution

$$|g^{(1)}(t)| = \int e^{-\Gamma t} G(\Gamma)\, d\Gamma \qquad (10)$$

where $G(\Gamma)$ is the normalized characteristic line-width distribution with $\bar{\Gamma}$ [$=\int G(\Gamma)\,\Gamma\, d\Gamma$] and μ_2 [$=\int(\Gamma - \bar{\Gamma})^2 G(\Gamma)\, d\Gamma$] being the average line width and the second moment of the characteristic line-width distribution. The variance (Var) is defined by $\mu_2/\bar{\Gamma}^2$. At concentrations $C \gg C^*$, the characteristic line width Γ measures a cooperative diffusion coefficient that can be related to the polymer mesh size (ξ).

III. Experimental Methods

III.1. Materials. The random copolymer poly(iBMA–tBAEMA) (lot CM1-120) was prepared by emulsion polymerization and purchased from Polyscience. The lot investigated was obtained from the latex-phase blend of several independent emulsion polymerizations. Therefore, the molecular weight distribution (MWD) might not necessarily be characteristic of a single free radical emulsion polymerization reaction and could be quite broad. Aqueous size-exclusion chromatography (SEC) provided an estimated of the copolymer weight-average molecular weight to be 2.7×10^6 g/mol. The aqueous SEC method involved conversion of methacrylate esters to methacrylic acid, followed by aqueous SEC with methacrylic acid calibration standards. Therefore, unlike organic solution SEC, the aqueous SEC method was thought to be independent of any possible polymer–polymer interactions present in SEC solutions of the methacrylate esters with organic solvents. The aqueous SEC value then is a valid candidate for comparison with weight-average MW values from very dilute solution studies by means of light scattering. The details will be discussed later in section IV. The molar ratio of iBMA to tBAEMA is 77:23 as determined by ^{13}C NMR. Random copolymers of poly(iBMA–tBAEMA) would certainly exhibit composition fluctuations that could influence the aggregation behavior. Thus, our study represents a development of the methodology and depicts the solution behavior of a specific poly(iBMA–tBAEMA). The quantitative nature of aggregation must depend on composition fluctuations.

The homopolymer poly(tBAEMA) was prepared by solution polymerization of monomer tBAEMA (Polyscience, Inc.) in THF at a concentration of 10% and 70 °C using 2,2′-azobis(isobutyronitrile) (Polyscience, Inc.) at 0.1% concentration as an initiator. The tBAEMA monomer was purified according to a normal procedure and vacuum distilled. The polymerization reaction was carried out under an argon atmosphere for 6 h. The polymer was then precipitated by adding a large amount of water and dried in a vacuum oven at 30 °C for 1 week.

The homopolymer of poly(iBMA) was purchased (Rohm and Haas Co.) after preparation by emulsion polymerization (lot 39015-23); the weight-average molecular weight is approximately 1.7×10^6 g/mol by SEC and LS.

III.2. Solution Preparation. Dilute solutions were prepared by dissolving the copolymer in freshly distilled solvents that were of high purity (Aldrich Chemical Co.). Semidilute solutions were prepared in the same way, except that after dissolution, the solutions were allowed to reach equilibrium over a period of another month with occasional agitation of the semidilute polymer solutions. Dust particles were allowed to settle in semidilute solutions over long periods of time (weeks to months). The solutions were clarified further by centrifugation for 4 h at 3000–5000 gravity. The clarified solutions were then carefully transferred to precleaned dust-free light-scattering cells by means of precleaned dust-free pipettes. For

Table I
Molecular Parameters of Poly(iBMA-tBAEMA) in Different Solvents[a]

	IPA	TMEDA	DMF	DMAA	TMEDA/HTN[b]
ν_A	0.125	0.074	0.049	0.043	
ν_B	0.128	0.073	0.049	0.040	
ν	0.124	0.075	0.051	0.045	0.072
n_0	1.368	1.412	1.428	1.433	1.409
M_w, 10^6 g/mol	2.42	5.86	8.52	9.08	13.6
R_g, nm	95	131	151	162	205
R_h, nm	65	100	115	120	152
R_h/R_g	0.69	0.77	0.76	0.74	0.74
10^3C^*, g/mL	4.69	4.33	4.11	3.55	

[a] Abbreviations: A, poly(iBMA); B, poly(tBAEMA); n_0, refractive index of solvent; IPA, isopropylamine; TMEDA, *N,N,N',N'*-tetramethylethylenediamine; DMF, *N,N*-dimethylformamide; DMAA, *N,N*-dimethylacetamide; HTN, 3-heptanone. Temperature: 30 °C. [b] Compositions of TMEDA/HTN: mole ratio of TMEDA/HTN = 0.4/0.6.

dilute copolymer solutions, a PTFE (Teflon) membrane filter (Millipore Co.) with 0.5-μm pore diameter was used to investigate the filtration effect (see IV.1.d).

III.3. Differential Refractometry. Refractive index increments (ν) were measured by means of a Brice Phoenix differential refractometer. The refractometer cell could be controlled to ±0.02 °C. Values of ν at 488 nm and 30 °C were interpolated from those values measured at 436 and 546 nm and the same temperature. The interpolated results (measured mostly to ±0.001) for the two homopolymers, poly(iBMA) and poly(tBAEMA), as well as the copolymer, poly(iBMA-tBAEMA), in different solvents are listed in Table I.

III.4. Light Scattering. A standard laboratory-built light-scattering spectrometer was used to measure the scattered intensity by photon counting and time correlation function by using a Brookhaven Instruments BI-2030 128-channel digital autocorrelator over an angular range of 15° to 135°. LLS measurements were performed at 30 ± 0.05 °C by using a Spectra Physics argon ion laser (Model 165) operating at λ_0 = 488 nm and an output power of 0.1 W.

IV. Results and Discussion

In this section, we shall proceed to discuss our experimental results from a chronological order, i.e., according to our development of LLS studies of the copolymer. Thus, we start with the dilute solution behavior (IV.1). By taking advantage of the fact that the copolymer had essentially isorefractive components with *different* chemical properties, we could determine the *true* molar mass of the aggregates in the dilute solution regime. Semidilute solution behavior (IV.2) was investigated to learn some aspects of intermolecular interactions of the aggregates. Finally, we performed experiments at very dilute solution concentrations (IV.3) in order to show experimentally how the aggregates can be taken apart by dilution and can be reduced to the isolated coil state at very low concentrations as in the case of micelles.

IV.1. Dilute Solution Behavior. a. Refractive Index Increments. Table I lists the refractive index increments of poly(iBMA), poly(tBAEMA), and poly(iBMA-tBAEMA) in isopropylamine (IPA); *N,N,N',N'*-tetramethylethylenediamine (TMEDA); *N,N*-dimethylformamide (DMF); *N,N*-dimethylacetamide (DMAA); and a solvent mixture of TMEDA and 3-heptanone (HTN) with a molar ratio of [TMEDA]/[HTN] = 0.4/0.6 at λ_0 = 488 nm and 30 °C. A very important finding for this copolymer is that the two homopolymers (poly(iBMA) and poly(tBAEMA)) are essentially isorefractive with $\Delta \equiv \Delta\nu = \nu_A - \nu_B \simeq 0.003, 0.001, 0$, and 0.003 in IPA, TMEDA, DMF, and DMAA, respectively. The measured values of ν for the copolymer agree with the computed ones to with ~0.002, ~0.001, ~0.002, and ~0.003 for poly(iBMA-tBAEMA) in IPA, TMEDA, DMF, and DMAA, respectively. Thus, in the worst case, we have

$$\Delta M_w \simeq \Delta M_{app} \simeq 2(P/\nu) \times 3 \times 10^{-3} + Q\left(\frac{3 \times 10^{-3}}{\nu}\right)^2 \quad (5a)$$

If we let $\delta W_{iA} = \overline{\delta W_{iA}} = 1$, corresponding to 100% fluctuation in the composition, we can rewrite eq 5a to get

$$\frac{\Delta M_w}{M_w} \simeq 6 \times 10^{-3}/\nu + 18 \times 10^{-6}/\nu^2 \lesssim 10^{-1} \quad (5b)$$

which implies that measurements of M_{app} yield essentially the true M_w and that uncertainties in our refractive index increment measurements between the two homopolymers and the copolymer can account for variations of only 10% or less and certainly not by factors of 2–5. The isorefractive approximation of segments of iBMA and tBAEMA in poly(iBMA-tBAEMA) forms the key to interpreting the light-scattering results of our interacting copolymer solutions, as we are no longer concerned with apparent molecular weight or apparent radius of gyration problems.

b. Light-Scattering Intensity Measurements. According to eq 2, the angular distribution of absolute scattered intensity for the "isorefractive" copolymer (here we refer to "isorefractive" for the two-component segments iBMA and tBAEMA in poly(iBMA-tBAEMA), not between poly(iBMA-tBAEMA) and the solvents) in dilute solution can be plotted by using the Zimm approach to get M_w, R_g, and A_2. Figure 1 shows the Zimm plots for poly(iBMA-tBAEMA) in the four pure solvents we have studied: (a) IPA, (b) TMEDA, (c) DMF, and (d) DMAA. We present the four Zimm plots to demonstrate the appearance of typical normal scattering behavior that one encounters in homopolymer solutions. The macromolecular parameters determined by the Zimm plots are listed in Table I. For each solvent, we have also computed the overlap concentration C^* to show that the extrapolation to "infinite" dilution was performed at $C \ll C^*$. However, on closer examination of values of the molecular weight (M_w) for poly(iBMA-tBAEMA) in the four solvents, the apparent molecular weight M_{app} changed from 2.42×10^6 to 9.08×10^6 g/mol. Here we consider the determined molecular weights first as M_{app}s because we are dealing with a copolymer. However, the variation of molecular weight by a factor of more than 3 would be difficult to take into account on the basis of estimates of eq 5b alone. We have noted the larger uncertainties in ν_A and ν_B for the copolymer in DMF and DMAA. Variation of M_{app} could again be detected by adding 3-heptanone to TMEDA, i.e., for poly(iBMA-tBAEMA) in a mixed solvent (TMEDA/HTN), although the solvent mixture (TMEDA/HTN) could add another complication of preferential solvent absorption to the data interpretation. Similar refractive indices of TMEDA and of HTN with n_0 = 1.412 and 1.405, respectively, as revealed by ν = 0.075 and 0.072 for TMEDA and TMEDA/HTN, respectively, suggest that only a small possible effect could be attributed to preferential solvent absorption, if any. Yet, M_{app} changed from 5.86×10^6 g/mol in TMEDA to 1.36×10^7 g/mol in TMEDA/HTN. Consequently, we can consider the molecular weight determination of poly(iBMA-tBAEMA) by light scattering to be M_w instead of M_{app}. The difference in M_w (or more precisely defined as the molar mass for the aggregated copolymer) from 2.42×10^6 to 1.36×10^7 g/mol suggests polymer aggregation properties in different solvents with no guarantee

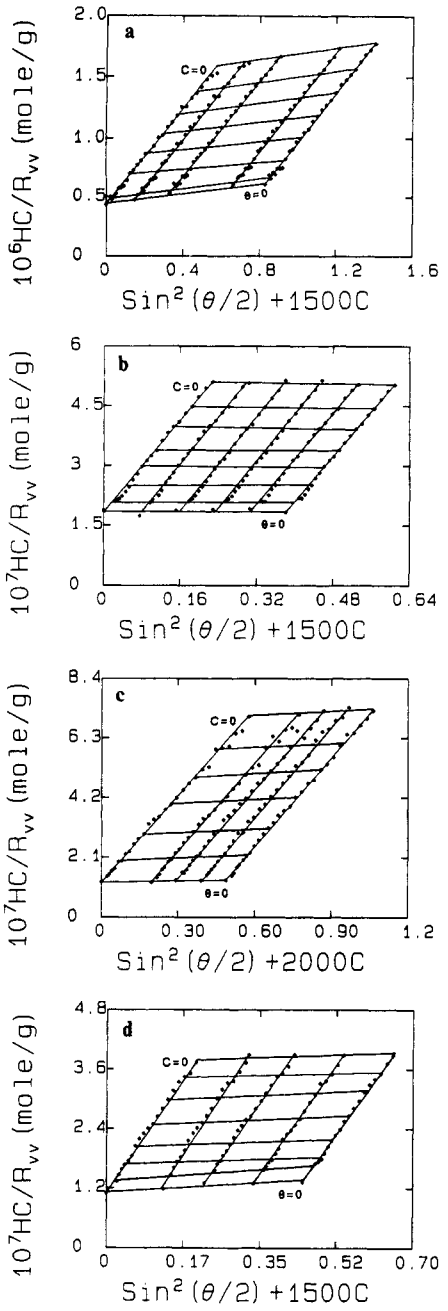

Figure 1. (a) Zimm plot of poly(iBMA-tBAEMA) in isopropylamine (IPA) at 30 °C: $C_1 = 1.11 \times 10^{-4}$ g/mL, $C_2 = 2.21 \times 10^{-4}$ g/mL, $C_3 = 4.43 \times 10^{-4}$ g/mL, and $C_4 = 5.53 \times 10^{-4}$ g/mL. (b) Zimm plot of poly(iBMA-tBAEMA) in *N,N,N',N'*-tetramethylethylenediamine (TMEDA) at 30 °C: $C_1 = 5.09 \times 10^{-5}$ g/mL, $C_2 = 1.02 \times 10^{-4}$ g/mL, $C_3 = 1.53 \times 10^{-4}$ g/mL, $C_4 = 2.04 \times 10^{-4}$ g/mL, and $C_5 = 2.55 \times 10^{-4}$ g/mL. (c) Zimm plot of poly(iBMA-tBAEMA) in *N,N*-dimethylformamide (DMF) at 30 °C: $C_1 = 4.88 \times 10^{-5}$ g/mL, $C_2 = 9.76 \times 10^{-5}$ g/mL, $C_3 = 1.46 \times 10^{-4}$ g/mL, and $C_4 = 1.95 \times 10^{-4}$ g/mL. (d) Zimm plot of poly(iBMA-tBAEMA) in *N,N*-dimethylacetamide (DMAA) at 30 °C: $C_1 = 7.47 \times 10^{-5}$ g/mL, $C_2 = 1.50 \times 10^{-4}$ g/mL, $C_3 = 2.24 \times 10^{-4}$ g/mL, and $C_4 = 2.99 \times 10^{-4}$ g/mL.

that $M_w \simeq 2.42 \times 10^6$ g/mol is the true molecular weight of the unaggregated poly(iBMA-tBAEMA) sample. The other values of M_w are all for poly(iBMA-tBAEMA) with different degrees of aggregation due to the nature of solvent quality for the two components of the copolymer and the composition/structure distribution of the two components within each copolymer chain of length i; i.e., the compositional drift of comonomer ratio as a function of molecular weight is characteristic of free radical copolymerization with comonomers of divergent reactivity ratios.

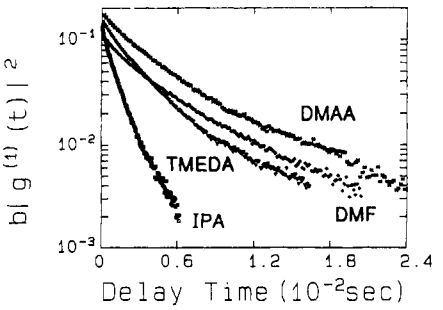

Figure 2. Semilog plots of net time correlation function of poly(iBMA-tBAEMA) in IPA (hollow squares), TMEDA (hollow triangles), DMF (hollow diamonds), and DMAA (stars) at 30 °C. The experimental conditions and fitting results are listed in Table III.

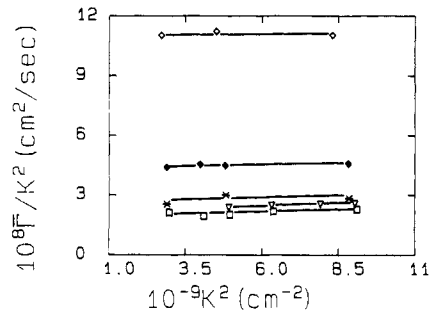

Figure 3. Plots of $\bar{\Gamma}/K^2$ versus K^2 for poly(iBMA-tBAEMA): in IPA (hollow diamonds), $C = 4.43 \times 10^{-4}$ g/mL; TMEDA (solid diamonds), $C = 3.44 \times 10^{-4}$ g/mL; DMF (hollow triangles), $C = 1.46 \times 10^{-4}$ g/mL; DMAA (hollow squares), $C = 2.99 \times 10^{-4}$ g/mL; TMEDA/HPN (star, mole ratio = 0.4/0.6), $C = 4.64 \times 10^{-4}$ g/mL (at 30 °C by using a second-order cumulants fitting procedure).

The light-scattering intensity study of dilute poly(iBMA-tBAEMA) solutions leads us to the concept that the random copolymer poly(iBMA-tBAEMA) tends to form aggregates of varying degrees in most solvents. We could reach the above conclusion mainly because the copolymer had essentially isorefractive components (A = iBMA and B = tBAEMA). However, as random copolymers have segments of the A/B homopolymers of varying lengths, our use of eq 5b is approximate at best. So, we seek additional experimental evidence to confirm our supposition.

c. Dynamic Light-Scattering Measurements. From photon correlation measurements, the net intensity time correlation function, $b|g^{(1)}(\tau)|^2$, of the copolymer in IPA, TMEDA, DMF, and DMAA, as illustrated in Figure 2, shows an increase in the variance (Table III), with an increase in the degree of aggregation (i.e., the molecular weight of associated polymers in solution, as listed in Table I). However, except for the deviation from single exponential behavior, the net intensity–intensity time correlation function can be represented essentially by unimodal distributions. This behavior suggests that although some of the copolymers have aggregated, the degree of aggregation is not high in all of the solvents studied. In Table I, we have also noted that the values for the radius of gyration of the copolymer "aggregates" in both pure solvents and a TMEDA/HTN solvent mixture are fairly large, ranging from 95 to 205 nm. For the determination of the hydrodynamic radius, R_h, it is essential to exclude internal motions. Thus, $D^0(C)$ ($=\lim_{K\to 0} \bar{\Gamma}/K^2$) was obtained from plots of $\bar{\Gamma}/K^2$, as shown typically in Figure 3 for poly(iBMA-tBAEMA) in various solvents. The slope that is represented by a plot $\bar{\Gamma}/K^2$ ($\bar{\Gamma}/K^2 = D^0(C)(1 + fR_g^2K^2)$ with f being a dimensionless number dependent on chain structure, polydispersity, and sol-

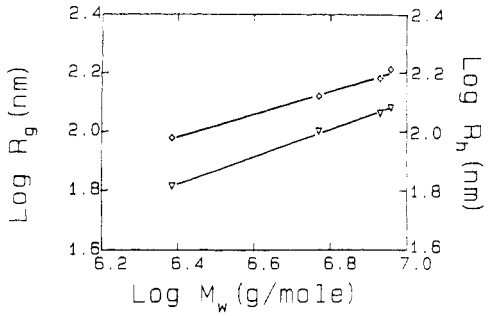

Figure 4. log–log plot of R_g (hollow diamonds) and R_h (inverted hollow triangles) versus M_w for poly(iBMA–tBAEMA) in different solvents (IPA, TMEDA, DMF, and DMAA). The plot assumes that the copolymer forms aggregates and that the conformation of aggregates remains the same. The α exponents suggest the nature of the aggregates as ideal coils, expanded coils, and hard spheres with α = 0.5, 0.6–0.7, and 0.33, respectively. The measured α values are 0.39 and 0.46, suggesting a less interpenetrating, spherelike, more compact coil conformation.

vent quality) versus K^2 is quite small. We have not extrapolated $D^0(C)$ to infinite dilution. At $C \sim 10^{-4}$ g/mL < C^*, we have assumed $k_dC \ll 1$ and $D_0{}^0 = \lim_{C\to 0} D^0(C) \simeq D^0(C)$ and used the Stokes–Einstein relation to compute an estimate of the hydrodynamic radius (R_h). The R_h values and the ratio of R_h/R_g are also listed in Table I. For a random coil, $R_h/R_g = 0.663$, while for an expanded coil, $R_h/R_g \simeq 0.58$. Thus, R_h/R_g values of 0.7–0.8 represent the polymer aggregate conformation to be somewhat more compact than even an ideal coil. If we take the notion that the polymer aggregates have comparable conformations, a log–log plot of R_g and R_h versus M_w should yield a scaling exponent, α_g (or α_h), following the relations

$$R_g = k_g M_w^{\alpha_g} \tag{11}$$

$$R_h = k_h M_w^{\alpha_h} \tag{12}$$

Figure 4 shows a log–log plot of R_g (and R_h) versus M_w with $\alpha_g \simeq 0.4$ and $\alpha_h \simeq 0.46$. The α exponent values are very rough estimates. Nevertheless, the values suggest a less interpenetrating spherelike coil conformation that is more compact than ideal coils, $\alpha_g \sim \alpha_h \simeq 0.6$, 0.5, and 0.34 for expanded, ideal, and globule coils, respectively. Figure 5 shows a long term equilibration behavior (in terms of 4–8 weeks) of poly(iBMA–tBAEMA) in different solvents. For solvents, acetone and TMEDA/HPN, $D^0(C)$ ($\simeq \Gamma/K^2$) increased slowly with time and leveled off after about 45 days. For IPA and DMAA, $D^0(C)$ remained relatively constant. For TMEDA, $D^0(C)$ decreased sharply and then leveled off after about 40 days. The values listed in Table I are equilibrium values. An increase in D signifies a decrease in R_h. The sharp decrease in D for the copolymer in TMEDA signifies polymer aggregation. It appears that the rate of formation of aggregates for the copolymer in different solvents are quite different, as shown in Figure 5. Furthermore, dissolution of such copolymers is a slow process.

d. Effect of Filtration. As we propose that the molecular weights of copolymer poly(iBMA–tBAEMA) in different solvents, as listed in Table I, could be attributed to preferential interactions of the two types of segments (made up of iBMA and tBAEMA monomers) of different length within the copolymer molecule, the intermolecular aggregation and possible intramolecular micellar formation should depend upon the local composition inhomogeneities in the random copolymer. If the above supposition is correct, fractions of the aggregated polymers should be separable from smaller size fractions by filtration. In a recent report by Galin,[7] apparent molecular weights ranging from (1.95–1.31) × 10^7 g/mol with R_g values of 220–560 nm for the same copolymer (same lot) were determined, while Potts et al.[8] reported apparent molecular weights of (2.53–6.42) × 10^6 g/mol in different solvents. The apparent molecular weight range reported by Galin is puzzling. The "M_{app}" values reported by Potts are of the same order of magnitude as the values listed in Table I. Here we need to make the following distinctions: (1) While Galin[7] and Potts et al.[8] considered their molecular weight determinations to be apparent, we showed that the apparent molecular weight determined was very close to the true molecular weight, i.e., $M_{app} \simeq M_w$, because the two homopolymers and the copolymer were essentially isorefractive. (2) As the variations in the molecular weight are not due to refractive index increment differences between the two components in the copolymer, the association behavior within the polymer chain (intramolecular interactions) and among the polymer chains (intermolecular interactions) could be the reason for this variation (see Figure 6). (3) Solution preparation procedures and the experimental scattering angular range covered could also be possible reasons for the disagreement, especially when compared with those reported by Galin. It is suffice to mention here that if the copolymer forms aggregates, we can demonstrate this association behavior by physically separating the larger particles from the smaller ones and then by redispersing the larger ones in a different solvent so as to show that the particle (associated copolymer) sizes depend on the local structures of the copolymer of composition j and chain length i, as well as the nature of the solvent.

Figure 7 shows a comparison of estimates of the hydrodynamic radius for poly(iBMA–tBAEMA) in DMAA by different solution preparation procedures, i.e., by centrifugation (denoted by curve a in Figure 7) and by filtra-

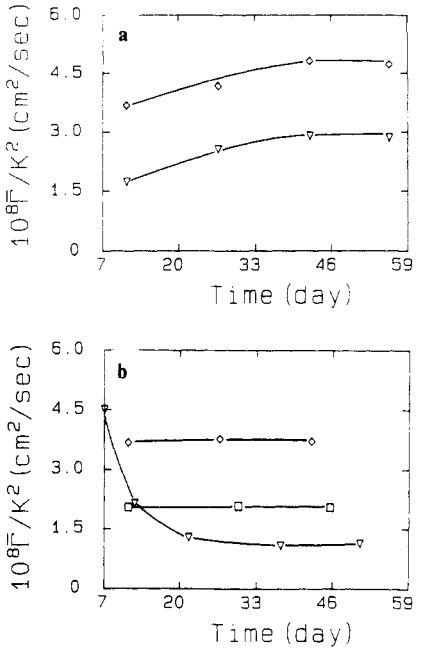

Figure 5. Time dependence of Γ/K^2 for poly(iBMA–tBAEMA) in different solvents at 25 °C and θ = 22°. (a) Hollow diamonds denote acetone (C = 4.41 × 10^{-4} g/mL) and hollow triangles, TMEDA/HPN (C = 4.64 × 10^{-4} g/mL). (b) Hollow diamonds denote IPA (C = 4.43 × 10^{-4} g/mL), hollow squares, DMAA (C = 2.99 × 10^{-4} g/mL), and hollow triangles, TMEDA (C = 1.02 × 10^{-4} g/mL). IPA curve is shifted down vertically by a factor of 3.

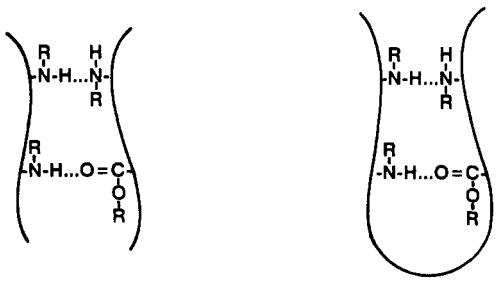

Figure 6. Schematic representation of intra- and intermolecular interactions of NRH.

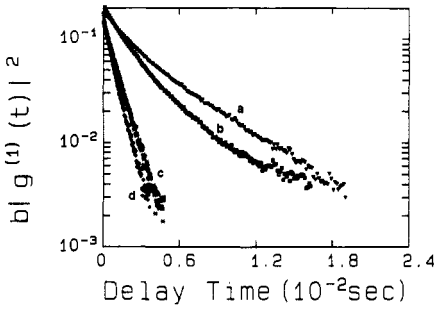

Figure 7. Filtration effect on time correlation function of a dilute solution of poly(iBMA–tBAEMA) at 30 °C and $\theta = 25°$: (a) in DMAA, $\bar{\Gamma} = 141\ s^{-1}$, $R_h = 115$ nm, Var = 0.23, $C = 1.79 \times 10^{-4}$ g/mL, by using centrifugation for solution clarification; (b) in DMAA, $\bar{\Gamma} = 220\ s^{-1}$, $R_h = 74$ nm, Var = 0.27, $C = 5.98 \times 10^{-4}$ g/mL, by using a 0.5-μM Millipore filter for solution clarification; (c) residue on 0.5-μm filter for poly(iBMA–tBAEMA) in DMAA, but redissolved in IPA, $\bar{\Gamma} = 513\ s^{-1}$, $R_h = 83$ nm, Var = 0.09, $C = 1.33 \times 10^{-4}$ g/mL; (d) poly(iBMA–tBAEMA) in IPA, $\bar{\Gamma} = 759\ s^{-1}$, $R_h = 57$ nm, Var = 0.19, $C = 1.11 \times 10^{-4}$ g/mL, by using centrifugation for solution clarification.

tion (denoted by curve b in Figure 7) using a 0.5-μm PTFE Millipore filter. Furthermore, we redissolved the residue on the 0.5-μm PTFE Millipore filter [from poly(iBMA–tBAEMA) in DMAA at $C = 5.98 \times 10^{-4}$ g/mL] in IPA (denoted by curve c in Figure 7) and compared the findings with the line-width results from a centrifuged dilute solution of poly(iBMA–tBAEMA) in IPA (denoted by curve d in Figure 7). As estimates on a qualitative scale, we have again ignored the concentration dependence of $\bar{D}^0(C)$ $(=\lim_{K\to 0} \bar{\Gamma}(C)/K^2)$. Curves a and b show comparable variances (0.23 versus 0.27) but quite different hydrodynamic radii (115 nm for the centrifuged solution in which some larger particles remained versus 74 nm for the solution which has been filtered by a 0.5-μm PTFE filter). Thus, the larger particles could be removed by filtration, and characterization of the copolymer could depend on solution preparation procedures. Reduction of the larger size particles from the overall sample size distribution changes the emphasis due to smaller size particles. Consequently, an increase in the variance after filtration is possible. Curve c represents the residue (from the filtration procedure) redissolved in IPA. Only large particles in DMAA could be excluded by the filter. However, after it was redissolved in IPA, $R_h \simeq 83$ nm with a variance of only 0.09. In comparison with $R_h \simeq 57$ nm from a centrifuged copolymer solution in IPA, the ratio of R_h for the copolymer in IPA and DMAA is $57/120 \sim 0.48$. Thus, $R_h \simeq 83$ nm in IPA corresponds to ~173 nm in DMAA; and 173 nm > 120 nm, in agreement with the expectation.

The second virial coefficient A_2 has a value of 12.2×10^{-5} cm^3 mol/g^2 for poly(iBMA–tBAEMA) in IPA but smaller values in solvents such as TMEDA, DMA, and DMAA. The decrease in A_2 values could be viewed as a weak supporting evidence on the quality of solvents. The aggregated copolymers in more compact forms should have smaller A_2 values when compared with the copolymer dissolved in IPA.

Table II
Preferential Solubility Classes by Permutation of Solubility (S) or Insolubility (I) of Component Homopolymers of the Copolymer Poly(iBMA–tBAEMA)

case	solubility class	homopolymer solubility	
		poly(iBMA)	poly(tBAEMA)
1	iBMA–tBAEMA (both)	S	S
2	iBMA (only)	S	I
3	tBAEMA (only)	I	S
4	iBMA–tBAEMA (neither)	I	I

Table III
Experimental Conditions for Dynamic Light Scattering Measurements in Dilute Solutions at 30 °C

	IPA	TMEDA	DMF	DMAA
concn, 10^{-4} g/mL	1.11	1.11	1.46	2.99
θ, deg	20	20	20	20
delay time increment $\Delta\tau$, μs	45	120	150	175
av line width $\bar{\Gamma}$, s^{-1} [a]	450	193	110	103
variance[a]	0.22	0.28	0.29	0.28
D $(=\bar{\Gamma}/K^2)$, 10^{-8} cm^2/s	12	4.9	2.7	2.5

[a] The results of data analysis were based on the second-order cummulants fit.

Our investigation of copolymer interaction with single solvents should consider that any solvent might be a monosolvent for one of the copolymer components. A permutation of all the possible solvent interaction classes of a solvent with a copolymer is listed in Table II.

A solution could be formed by a solvent for both comonomer components (Table II, case 1) or a solvent that was a nonsolvent for one of the two comonomer components (cases 2 and 3). For the rare case (4), there may be instances in which a nonsolvent for both comonomer components could produce a stable solution for the copolymer; the inverse case of two nonsolvents dissolving a homopolymer is well-known. Intra- and intermolecular polymer–polymer interactions between nonsolvated comonomer sequences might be expected for case 2 and 3 solutions. A priori, one might expect case 1 solutions to behave as homopolymer solutions and be relatively free of significant polymer–polymer interaction.

On the basis of the solubility determinations in the homopolymer analogs of the copolymer components, each of the solvents employed can be classified as case 1 solvents. Therefore, we believe that it is the nature of tBAEMA which introduces the additional interactions unique to this type of polymer additives.

IV.2. Semidilute Solution Behavior. In semidilute polymer solutions, the polymer coils (or its aggregated entities) overlap with one another. By following the format of eq 2, we can write

$$\frac{1}{R_{vv}(K)} \simeq \frac{1}{R_{vv}(0)}(1 + K^2L^2/3) \qquad (13)$$

where L is a correlation length denoting the extension of local concentration fluctuations. Figure 8 shows plots of $1/R_{vv}(K)$ versus $\sin^2(\theta/2)$ for poly(iBMA–tBAEMA) in TMEDA (a "poor" low polarity solvent) at 25 °C and at concentrations near C^* of 4.33×10^{-3} g/mL with $C = 2.07 \times 10^{-3}$ (curve a) and 1.41×10^{-2} g/mL (curve d). The data are in reasonable agreement with eq 13. From the initial linear slope, values of L decrease with increasing C at $C < C^*$ and approach a fairly constant value at

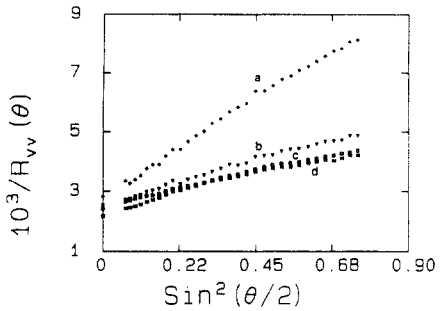

Figure 8. Angular dependence of scattered intensity of poly(iBMA-tBAEMA) in TMEDA at 25 °C: (a) $C = 2.07 \times 10^{-3}$ g/mL; (b) $C = 5.16 \times 10^{-3}$ g/mL; (c) $C = 8.24 \times 10^{-3}$ g/mL; (d) $C = 1.41 \times 10^{-2}$ g/mL.

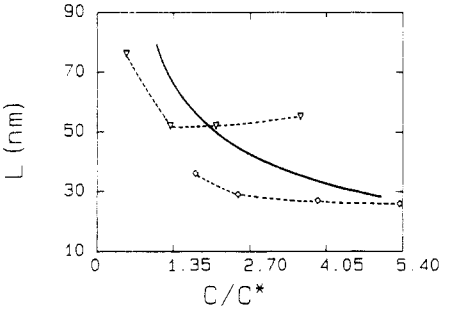

Figure 9. Concentration dependence of correlation length (L) of poly(iBMA-tBAEMA) in TMEDA (inverted hollow triangles, from Figure 7) and IPA (hollow diamonds) at 25 °C. L was calculated according to $1/R_{vv} = 1/R_{vv}(0)(1 + K^2L^2/3)$, showing different behavior from that of polystyrene in toluene at 25 °C (solid curve from: Chu, B.; Wu, D. *Macromolecules* **1987**, *20*, 1606).

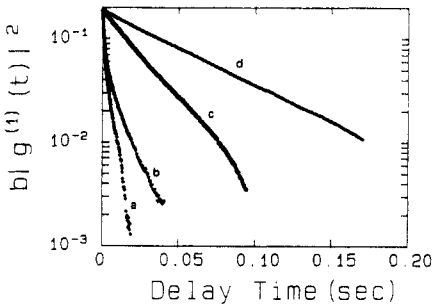

Figure 10. Measured net intensity-intensity time correlation function of poly(iBMA-tBAEMA) in TMEDA at 25 °C and $\theta = 25°$ with multiple delay time increments: a, TMEDA1, $\Delta\tau$ = 70, 70, 140, and 280 μs; b, TMEDA2, $\Delta\tau$ = 75, 150, 300, and 600 μs; c, TMEDA3, $\Delta\tau$ = 750 μs; d, TMEDA4, $\Delta\tau$ = 1340 μs.

$C > C^*$ as shown by the inverted hollow triangles in Figure 9. The same poly(iBMA-tBAEMA) in IPA (a "good" polar solvent) shows a similar leveling effect for L at $C > C^*$ (see hollow diamonds in Figure 9). In comparison with the concentration dependence of the correlation length L for polystyrene in toluene, as shown by the solid line in Figure 9, the leveling off of the correlation length supports the existence of less interpenetrating coils, as we have postulated in IV.1. For poly(iBMA-tBAEMA) in IPA, the correlation length is smaller and the plateau ratio for the copolymer in TMEDA and IPA is $(L_{TMEDA}/L_{IPA}) \sim 1.6$, which is comparable to the ratio $R_{g,TMEDA}/R_{g,IPA} \sim 1.4$, again suggesting less interpenetration among the more compact copolymer aggregated coils.

Figures 10 and 11 show time correlation function of poly(iBMA-tBAEMA) in TMEDA and IPA, respectively, at $\theta = 25°$ and 25° with multiple delay time increments. The time correlation function profile analysis of poly(iBMA-tBAEMA) in TMEDA with concentrations

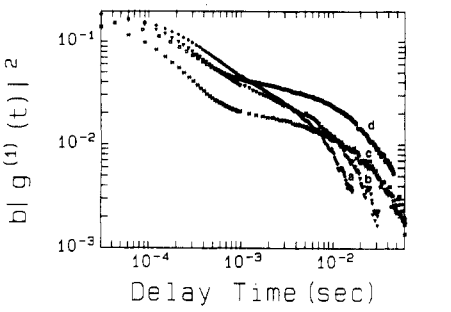

Figure 11. Measured net intensity-intensity time correlation function of poly(iBMA-tBAEMA) in IPA at 25 °C and $\theta = 25°$ with multiple delay time increments. a, IPA1, $\Delta\tau$ = 30, 60, 120, and 240 μs; b, IPA2, $\Delta\tau$ = 30, 120, 240, and 480 μs; c, IPA3, $\Delta\tau$ = 43, 172, 344, and 688 μs; d, IPA4, $\Delta\tau$ = 30, 240, 480, and 960 μs.

Table IV
Correlation Function Profile Analysis of Semidilute Solutions of Poly(iBMA-tBAEMA) in TMEDA and IPA by the CONTIN Method[a]

	TMEDA1	TMEDA2	TMEDA3	TMEDA4
10^3C, g/mL	2.07	5.16	8.24	14.1
C/C^*	0.52	1.3	2.1	3.6
θ, deg	25	25	25	25
$\bar{\Gamma}_1$, s^{-1}	1.0×10^2	75	20	8
$\mu_2/\bar{\Gamma}_1^2$	0.05	0.56	0.02	0.01
A_1	0.60	0.65		
$\bar{\Gamma}_2$, 10^2 s^{-1}	7.2	13		
$\mu_2/\bar{\Gamma}_2^2$	0.01	0.13		
A_2	0.40	0.35		
ξ, nm	38	21		

	IPA1	IPA2	IPA3	IPA4
10^3C, g/mL	8.16	11.7	18.5	25.1
C/C^*	1.7	2.5	3.9	5.4
θ, deg	25	25	25	25
$\bar{\Gamma}_1$, s^{-1}	96	55	33	25
$\mu_2/\bar{\Gamma}_1^2$	0.31	0.28	0.16	0.64
A_1	0.50	0.44	0.46	0.35
$\bar{\Gamma}_2$, 10^3 s^{-1}	3.0	3.8	4.7	5.6
$\mu_2/\bar{\Gamma}_2^2$	0.05	0.01	0.01	0.09
A_2	0.50	0.56	0.54	0.65
ξ, nm	13	10	8.5	7.1

[a] Temperature: 25 °C. $\xi = kT/(6\pi\eta_0 D_c)$; η_0(IPA) = 0.302; η_0(TMEDA) = 0.494.

Table V
Results of Dynamic Light Scattering and Data Analysis Based on the CONTIN Method for Very Dilute Solutions of Poly(iBMA-tBAEMA) in TMEDA at 30 °C

sample	concn, 10^{-5} g/mL	θ, deg	$\Delta\tau$, μs	$\bar{\Gamma}$,[a] s^{-1}	variance[a]	$\bar{D}$ $(=\bar{\Gamma}/K^2)$,[a] 10^{-8} cm^2/s
C1	44.5	20	120	212 (215)	0.36 (0.35)	5.32
C2	11.2	20	120	198 (200)	0.35 (0.33)	5.0
C3	5.56	20	120	(190)	(0.27)	(4.78)
C4	2.78	20	90	(224)	(0.43)	(5.62)
C5	0.927	20	120	2.5×10^2	0.79	6.3

[a] Values in parentheses were obtained by using a third-order cummulants fit. It makes no difference in analyzing $\bar{\Gamma}$ and variance of a dilute solution whether we use the CONTIN or the cummulants method, but for the extreme dilute case, only the CONTIN method could be used because of the large variance.

($C = 8.24 \times 10^{-3}$ and 14.1×10^{-3} g/mL) identical with those in Figure 8 shows unimodal decay time distributions for $C > C^*$, as listed in Table IV. In fact, curves c ($C = 8.24 \times 10^{-3}$ g/mL) and d ($C = 1.41 \times 10^{-2}$ g/mL) show single exponential behavior with a variance of only 0.01–0.02. The slow mode is a residual motion of some of the "free" copolymers in the pseudonetwork. At $C \lesssim C^*$, the time correlation functions of the copolymer in

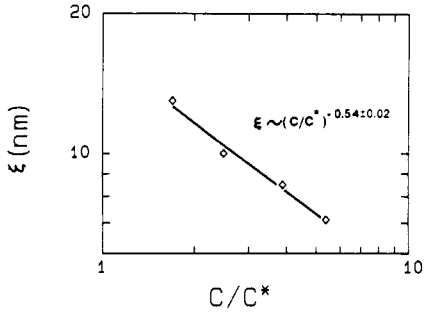

Figure 12. Concentration dependence of correlation length ξ of poly(iBMA-tBAEMA) in IPA. Experimental conditions are the same as in Figure 11. ξ was calculated by using the Stokes-Einstein relation $\xi = kT/(6\pi\eta_0 D_c)$ as well as the CONTIN method of data analysis, showing $\xi \propto (C/C^*)^{-0.54}$.

TMEDA for curves a and b in Figure 10 show bimodal decay time distributions with the area ratio $A_1/A_2 \sim 1.5$. In comparison with the time correlation functions of the copolymer in IPA, which is a better solvent than TMEDA for the copolymer because of a much lower value of M_w (2.42×10^6 g/mol instead of 5.68×10^6 g/mol as listed in Table I), the physical properties, such as the characteristic line width of the slow mode ($\bar{\Gamma}_1$) of the copolymer solution with TMEDA as the solvent, changes more drastically with increasing concentration; i.e., stronger interactions are present, leading toward more highly aggregated copolymers in TMEDA such that for $C/C^* \sim 2$, the copolymer aggregates in the semidilute solution become highly entangled. The unimodal behavior for curves c and d in Figure 10 also implies that our C/C^* values in Table IV are not to be taken literally. We can postulate our schematic model as follows.

When the copolymer is dissolved in IPA or TMEDA, some aggregates are formed because of intra- and intermolecular interactions between the copolymer and the solvent. The aggregation phenomenon, however, is dependent on concentration, since with increasing concentration, more copolymers could form aggregates because of inhomogeneity in the local polymer block length within each copolymer molecule. The copolymer that forms larger aggregates in TMEDA should, therefore, interact stronger in TMEDA with increasing concentration. As a consequence, the semidilute solutions of the copolymer in TMEDA should have effective C/C^* values lower than those listed in Table I, which assumes that the (aggregated) copolymer does not form additional new aggregates with increasing copolymer concentration. For the copolymer in IPA, the interactions are weaker. So, the slow mode decreases slower with increasing copolymer concentration. From the concentration dependence of the correlation length (or mesh size ξ), as shown in Figure 12, we get $\xi \propto (C/C^*)^{-0.54}$ for poly(iBMA-tBAEMA) in IPA; i.e., the exponent is less than the corresponding static correlation length $L \propto (C/C^*)^{-0.65\pm0.05}$ for polystyrene in toluene at 25 °C[9] even though we have used C^* in the copolymer solution to be a constant independent of concentration. The fact that the aggregated copolymers are less interpenetrating (which is equivalent to an expanded interpenetrating aggregated coil) could be one of the reasons for the decrease in the magnitude of the exponent as far as light scattering is concerned.

Figure 13 shows comparisons of time correlation functions at dilute and semidilute concentrations for poly(iBMA-tBAEMA) in IPA (a) and TMEDA (b) at 30 °C and $\theta = 25°$. The diamonds denote a unimodal characteristic line-width distribution with a variance of 0.18 for a dilute copolymer solution in IPA. With increasing concentrations, the triangles (IPA2) and squares (IPA4) show

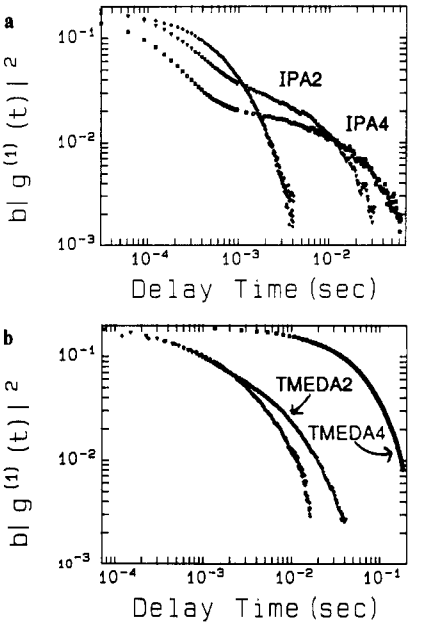

Figure 13. (a) Comparison of time correlation function at dilute and semidilute concentrations for poly(iBMA-tBAEMA) in IPA at 30 °C and $\theta = 25°$: diamonds denote $C = 1.11 \times 10^{-4}$ g/mL, $\Delta\tau = 30$ μs, $\bar{\Gamma} = 760$ s^{-1}, Var = 0.18; triangles IPA2; squares IPA4 as in Figure 11. (b) Comparison of time correlation function at dilute and semidilute concentrations for poly(iBMA-tBAEMA) in TMEDA at 30 °C and $\theta = 25°$: diamonds denote $C = 1.1 \times 10^{-4}$ g/mL, $\Delta\tau = 120$ μs, $\bar{\Gamma} = 289$ s^{-1}, Var = 0.28; triangles TMEDA2; squares TMEDA4 as in Figure 10.

unambiguous bimodal characteristic line-width distributions, signifying the presence of polymer entanglement, as well as the polydisperse characteristics of the copolymer aggregates. The effective b value (eq 7) decreases with increasing concentration as the copolymer semidilute solutions become more homogeneous with increasing concentration. Figure 13b shows quite a different characteristic. While a dilute solution of poly(iBMA-tBAEMA) in TMEDA, as denoted by diamonds, shows a unimodal characteristic line-width distribution with a variance of 0.28, the semidilute solution (trianges for TMEDA2 with $C/C^* \sim 1.3$ and $C \sim 5.16 \times 10^{-3}$ g/mL) shows a transition to a bimodal characteristic line-width distribution and eventually forms a pseudonetwork with mostly entangled polymer aggregates, as denoted by squares for TMEDA4 with $C/C^* \sim 3.6$ and $C \sim 14.1 \times 10^{-3}$ g/mL. The increasing interactions of the copolymer with increasing concentration in TMEDA is clearly demonstrated by the disappearance of the bimodal characteristics for poly(iBMA-tBAEMA) in TMEDA. Over the same C/C^* range, the bimodal characteristics clearly remain for the same poly(iBMA-tBAEMA) in IPA, as shown in Figure 13a.

IV.3. Very Dilute Solution Behavior. With our supposition of interacting copolymers to form coil surface or unentangled supramolecular aggregates in the solvents we have studied, we proceed, in this section, to test this postulate by making laser light scattering measurements at very dilute concentrations. The idea is that if the copolymers, like micelles, form aggregates at dilute concentrations, we may be able to observe a breaking up of those aggregates at very low concentrations.

Figure 14 shows plots of excess scattered intensity of poly(iBMA-tBAEMA) at 30 °C and after extrapolation to $\theta = 0$ in DMAA (inverted triangles) and in TMEDA (squares). Unfortunately, our light-scattering intensity data at very dilute concentrations were not sufficiently precise to permit an unambiguous extrapolation for deter-

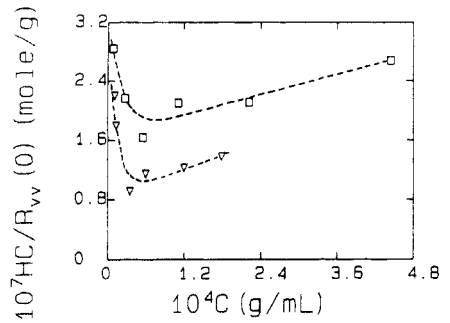

Figure 14. Dilution effect on excess scattered intensity of poly(iBMA-tBAEMA) at 30 °C and after extrapolation to $\theta = 0°$ in DMAA (triangles) as in TMEDA (squares). The molecular weight could be estimated by extrapolation to infinite dilution from the upward curve and the downward curve, respectively. However, we could not establish a precise end point ($\lim_{C\to 0} HC/R_{vv}$) with the present data. It is clear that M_w should be $\lesssim 2.4 \times 10^6$ g/mol.

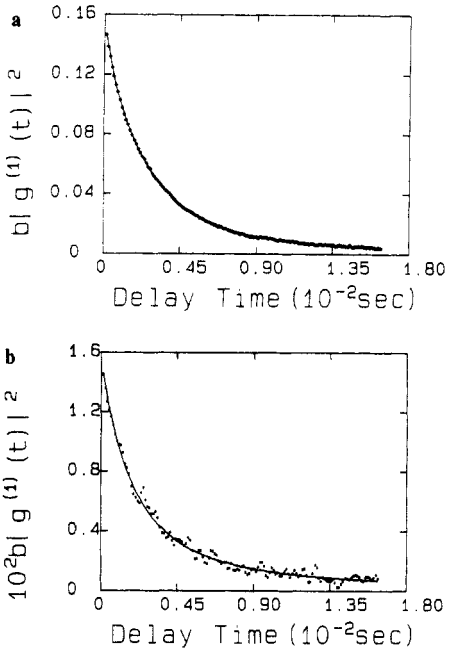

Figure 15. Dilution effect on time correlation function for poly(iBMA-tBAEMA) solution in TMEDA at 30 °C and $\theta = 20°$. Here are two typical time correlation functions: (a) $C = 1.12 \times 10^{-4}$ g/mL; (b) $C = 9.27 \times 10^{-6}$ g/mL. Diamonds and squares are experimental data. The solid lines represent CONTIN fitting curves. The fitting results are listed in Table V.

mination of the copolymer weight-averaged molecular weight in its unaggregated state. A rough estimate by eye inspection would suggest $M_w \lesssim 2.4 \times 10^6$ g/mol. Extrapolation of HC/R_{vv} from the downward section of the curve at higher (but dilute) concentrations would yield M_w values comparable to those listed in Table I. These are clearly M_w values for aggregated copolymers, and the degree of aggregation depends on solvent quality. The upward bend and their extrapolation to about the same end point ($\lim_{C\to 0} HC/R_{vv}$ = same) in the scattering plot of HC/R_{vv} versus C have provided us very strong evidence on the supramolecular formation of poly(iBMA-tBAEMA) in TMEDA and in DMAA.

Figure 15 shows the dilution effect on the time correlation function for poly(iBMA-tBAEMA) in TMEDA at 30 °C and $\theta = 20°$, with (a) denoting $C = 1.12 \times 10^{-4}$ g/mL and (b) denoting $C = 9.27 \times 10^{-6}$ g/mL. It is interesting to note a corresponding drop in the effective b value (eq 7) as shown in Figure 15b. At very dilute concentrations, we have also noted an increase in the average D value, which signifies a decrease in the hydrodynamic radius and a broader line-width distribution, as shown in Figure 16. The absolute magnitude is not sufficiently precise to render a quantitative analysis. Nevertheless, we can see that breakup of the supramolecular aggregates upon excessive dilution signifies that under normal dilute concentrations we have aggregation present in both the good and poor poly(iBMA-tBAEMA)/solvent systems.

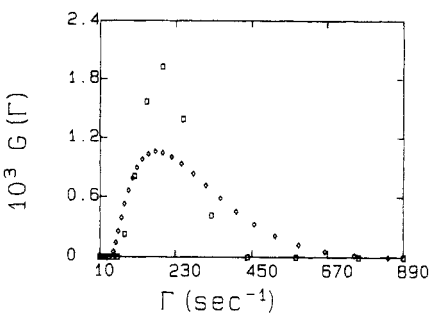

Figure 16. Dilute effect on average line-width distribution function of poly(iBMA-tBAEMA) in TMEDA (from Figure 15). Diamonds denote $C = 9.27 \times 10^{-6}$ g/mL and squares, $C = 1.12 \times 10^{-4}$ g/mL.

V. Conclusions

Poly(iBMA-tBAEMA) forms supramolecular aggregates in most solvents, such as TMEDA, DMAA, etc. The aggregates enhance the effectiveness of the polymer additive because, in the presence of polymer aggregation, entangled polymer pseudonetworks are formed at lower overlap concentrations. The non-Newtonian fluid behavior for the supramolecular polymer solution is responsible for such copolymers to be useful as effective additives.

By taking advantage of the almost isorefractive coincidence of poly(iBMA), poly(tBAEMA), and poly(iBMA-tBAEMA), we could ascertain the determination of the weight-averaged molar mass and the z-averaged radius of gyration for the supramolecular polymer solutions by light scattering intensity measurements. It should be noted that even if the refractive index increments of poly(iBMA), poly(tBAEMA), and poly(iBMA-tBAEMA) were identical, as we have demonstrated experimentally to within our measurement uncertainties, there should be no guarantee of the same refractive index increment for local segments of iBMA and tBAEMA having varying lengths in the copolymer. However, this aggregation behavior was further confirmed by physically separating the aggregates and subsequent dissolution of the residue in a different solvent. When we combine static light scattering with dynamic light scattering, we note that the aggregated polymers form less interpenetrating and relatively compact coils and that the degree of aggregation increases with polymer concentration. Finally, the aggregation phenomenon can be shown unambiguously by carrying out laser light scattering measurements at very dilute concentrations. A breakup of the aggregates clearly suggests that in the normal dilute solution regime, we determine the molar mass of the aggregates (instead of the molecular weight of the copolymer). The copolymer poly(iBMA-tBAEMA) behavior can be generalized to other copolymer systems. With our understanding on how the polymer coils aggregate, better polymer additives can be designed.

Acknowledgment. We gratefully acknowledge support of this work by this U.S. Army Research Office (DAAL0387K0136).

References and Notes

(1) Hong, S. H.; McHugh, V. M. Review of polymerization and properties of aminoalkyl acrylates and aminoalkyl methylacrylates, with 31 references. NTIS No. ADA 197705, July 1988.
(2) Hong, S. H.; McHugh, V. M. Review of preparation and properties of polymers from copolymerization of aprotic acrylic monomers with protic acrylic monomers, with 57 references. NTIS No. ADA 197467, July 1988.
(3) Debye, P. *J. Phys. Colloid Chem.* **1947**, *51*, 18.
(4) Stockmayer, W. H.; Moore, L. D., Jr.; Fixman, M.; Epstein, B. N. *J. Polym. Sci.* **1955**, *16*, 517.
(5) Bushuk, W.; Benoit, H. *Can. J. Chem.* **1958**, *36*, 1616.
(6) Chu, B.; Ying, Q.; Lee, D.; Wu, D. *Macromolecules* **1985**, *18*, 1962. See references therein.
(7) Galin, J. C. *Report on Copolymers CM, K-125E and K-125G*; ICS: Strasbourg, France (private communication).
(8) Potts, M. K.; Hagnauer, G. L.; Dunn, D. A., private communication.
(9) Chu, B.; Wu, D. *Macromolecules* **1987**, *20*, 1606.

Registry No. Poly(iBMA-tBAEMA), 40008-96-6.

Miscibility of Poly(ethylene oxide) and Poly(styrene-*co*-acrylic acid) Blends

Won Ho Jo* and Sang Cheol Lee

Department of Textile Engineering, Seoul National University, Seoul 151-742, Korea.

Received July 5, 1989; Revised Manuscript Received October 25, 1989

ABSTRACT: The miscibility for blends of poly(ethylene oxide) (PEO) with poly(styrene-*co*-acrylic acid) (SAA) was examined as a function of the comonomer content of the copolymer. PEO was found to be miscible with SAA copolymers having an acrylic acid content higher than 7 mol %. The segmental interaction parameters were determined by combining the equilibrium melting point depression and a binary interaction model. These values suggest that both the specific interaction between ethylene oxide and acrylic acid segments and the intramolecular repulsive force in SAA copolymer are responsible for the miscibility. The minimum acrylic acid content in SAA for the blend to be homogeneous was predicted to be 7.7 mol % from the binary interaction model and the calculated values of segmental interaction parameters.

Introduction

In recent years, the origins of miscibility between polymer pairs have been understood based on theoretical backgrounds and experimental results.[1,2] Thermodynamically, polymer–polymer miscibility requires a negative heat of mixing. Therefore, miscible blends will be formed if there are some specific intermolecular interactions between polymer pairs such as hydrogen bonding, etc.[3]

On the other hand, many random copolymers have been reported to be miscible with homopolymers in spite of the absence of specific interactions.[4-8] In order to interpret this phenomenon, Kambour et al.[9] proposed a binary interaction model for mixtures of a homopolymer and a random copolymer based on the Flory–Huggins lattice model. According to this model, the mutual repulsive force between dissimilar segments in the copolymer can lead to the negative heat of mixing necessary to attain miscibility. More recently, Paul et al.,[10-14] Karasz et al.,[15,16] and others[17-19] have further extended the above binary interaction model to several types of blends containing copolymers and applied the model to interpret the effect of the copolymer composition on the miscibility of blends.

According to the binary interaction model, miscible blend systems can be developed by designing copolymers through appropriate choices of comonomers and copolymer compositions. Besides the mutual repulsive force between dissimilar segments in the copolymer, some specific interactions between polymer pairs also play an important role for inducing miscibility. Considering the above two factors, in this study the acrylic acid (AA) was incorporated onto polystyrene (PS) to enhance the miscibility of poly(ethylene oxide) (PEO) and polystyrene. The primary objectives of this study are (1) to investigate the effect of copolymer composition on the miscibility, (2) to determine the segmental interaction parameters by combining the binary interaction model and the data obtained by analysis of the equilibrium melting point depression, (3) to ascertain which interactions are responsible for the miscibility, (4) to predict the critical copolymer composition for the mixture to be miscible, and (5) to clarify the nature of the specific intermolecular interactions by using spectroscopic analysis.

Experimental Section

Materials. Poly(ethylene oxide) ($M_w = 1.0 \times 10^5$, $T_g = -56$ °C) was obtained from Aldrich Co. It was used as received without further purification. The poly(styrene-*co*-acrylic acid) (SAA) was synthesized in a sealed glass ampule by bulk polymerization at 60 °C, using benzoyl peroxide as an initiator. The copolymer formed was isolated by pouring the reaction mixture into *n*-hexane and dried in a vacuum oven at 100 °C for 2 days. The maximum degree of conversion was controlled to about 7 wt %. The acrylic acid content of the copolymer was determined by titration in benzene/methanol (9/1, v/v) with a standardized methanolic NaOH solution using phenolphthalein as an indicator. The intrinsic viscosity was measured at 25 °C in dilute tetrahydrofuran solution by extrapolation to zero concentration. The copolymer composition and other properties are listed in Table I.

Preparation of Blends. The blends were prepared by dissolving the component polymers in benzene/methanol (9/1, v/v). The solutions were cast on an aluminum dish, and most of solvent was allowed to evaporate slowly in the air at room temperature. The resulting films were then completely dried in a vacuum oven at 60 °C for at least 3 days.

0024-9297/90/2223-2261$02.50/0